JOURNAL OF MATERIALS SCIENCE 27 (1992) 5073–5083

Strength of vibration-welded modified polyphenylene oxide structural foam butt joints

V. K. STOKES
GE Corporate Research and Development, Schenectady, NY 12301, USA

Tensile tests on 120 Hz vibration-welded butt joints of specimens cut from 6.35 mm thick plaques of modified polyphenylene oxide (M-PPO) structural foam have shown that 5% and 25% density reduction M-PPO structural foams weld well. This has been shown to be true for both foam-to-foam and skin-to-foam welds. The weld process phenomenology for these foams is shown to be identical to that for all neat resins: the penetration–time curve exhibits the four phases associated with vibration welding. The effect of weld pressure is not as significant as for solid M-PPO, for which increases in weld pressure are known to cause large decreases in weld strength.*

1. Introduction

In vibration welding of thermoplastics, frictional work done by vibrating two parts under pressure, along their common interface, is used to generate heat to effect welds [1]. Past work on welding [1–4] has focused on characterizing the effects of weld parameters, such as the weld frequency, the weld amplitude, the weld pressure, and the weld time, on the welding process and the strength of welds for several different thermoplastics. That work has shown that the most important parameter affecting weld strength is the weld penetration, which is the decrease in distance between parts being welded that is caused by lateral outflow of material in the molten film. Very high weld strengths can be achieved when the penetration exceeds a critical threshold; the weld strength drops off for penetrations below this value. This threshold is affected by the thickness of the part being welded; the threshold increases with part thickness [5]. The weldability of dissimilar amorphous polymers and the weldability of amorphous to semicrystalline polymers have been discussed previously [6, 7], and the effects of chopped glass fillers on the weld process and weld strength have also been reported [8].

This paper discusses the vibration welding of modified polyphenylene oxide structural foams (M-PPO-SF). (Modified polyphenylene oxide is a blend of poly(2,6-dimethyl-1,4-phenylene ether) and high-impact polystyrene.) The M-PPO-SF used in this study was 6.35 mm (0.25 in) thick Noryl® FN215 at density reductions of 5% and 25%. All the welds in this study were done at a fixed weld frequency of 120 Hz and a weld amplitude of 1.59 mm (0.0625 in) at two different weld pressures.

Because the mechanical behaviour of structural foams is very different from that of the resins from which they are made, and the relevance of such differences to the interpretation of weld strength data, a brief overview on foams and mechanical property data for 25% density reduction M-PPO-SF is given below.

2. Structural foams

Rigid thermoplastic structural foams are used for moulding thin-walled structural parts, either by the expansion of dissolved gases in the molten plastic or by gases generated by a chemical reaction during the moulding process. The morphology of a foam part consists of flat "solid" outer skins surrounding a porous inner core, resulting in light structural components that have relatively high strength-to-weight ratios. Because of the complex morphology, these materials do not have the usual mechanical properties associated with homogeneous materials. Rather, for these material systems, standard tests, such as tensile and flexural tests, measure system properties that depend not only on the foam but also on the test-specimen geometry and the type of test [9]. As a result, if the material is assumed to be homogeneous, the measured "effective" flexural modulus can be 50% larger than the effective tensile modulus [10].

Rigid structural foams are described in terms of a general, density reduction level due to foaming. That level of "normal" density reduction is controlled by the process parameters and is directly related to the amount of material injected into the mould. The actual local density reduction and the local mechanical properties vary over a part [10].

Much of the literature on the mechanical properties of foams is concerned with relating the flexural modulus of a rectangular beam to the foam density. It has been suggested [11] that this "flexural modulus" can be simply related to the macroscopic average density of the foam. Also, a relationship between the local (through-thickness) modulus and the local (through-thickness) density has been used to predict the "flexural modulus" [12, 13]. However, such a dependence

* Based on a paper presented at The Society of Plastics Engineers 49th Annual Technical Conference in Montreal, Canada.

0022–2461 © *1992 Chapman & Hall*

of the local modulus on the local density is difficult to measure. Also, there is some question as to the meaning of a pointwise local density for structural foams, which can have rather large pores.

Because the properties of foams vary across a part and because standard tests used for determining the mechanical properties of homogeneous materials do not determine material properties of nonhomogeneous materials, the choice of test specimens and test procedures is important, as is the question of how experimental data are to be used for predicting part performance. These issues have been addressed [9, 10], and new test procedures have been defined, and data for 5% and 15% density reduction M-PPO-SF given. Because of the relevance to this welding study, data for 25% density reduction foam will be discussed in some detail.

The "mechanical properties" of the 25% density reduction material were obtained by tests on eighteen 152.4 mm × 19.05 mm × 6.35 mm (6 in × 0.75 in × 0.25 in) bars cut from 152.4 mm × 457.2 mm × 6.35 mm (6 in × 18 in × 0.25 in) edge-gated moulded plaques, with the flow direction along the length. The eighteen bars were numbered 1–18, with Specimen 18 being the closest to the gated edge, as shown schematically in Fig. 1. Details of the new standardized test procedures used for obtaining the data for the 25% density reduction material, including the measurement of the average densities of the specimens, their elastic moduli, and their ultimate stresses and strains, have been given earlier [9]. Essentially, the average density, ρ, is the mass of each 152.4 mm × 19.05 mm × 6.35 mm bar divided by its volume. The tensile and bending moduli, E_{TR} and E_{BR}, respectively, are the numbers obtained by interpreting tensile and three-point bend test data in terms of homogeneous material theory. That is, E_{TR} and E_{BR} are the equivalent homogeneous material moduli.

Fig. 2 shows the measured values of ρ, E_{TR} and E_{BR} as a function of the specimen number. The average density, ρ, varies significantly along the plaque, from 0.73 g cm^{-3} for Specimen 1, to 0.91 g cm^{-3} for Specimen 18, as do the tensile and bending moduli E_{TR} and E_{BR}, respectively. This shows that nominal density reduction, 25% in this case, is not a good indicator of the local density. Notice that the variations in E_{TR} and E_{BR} appear to track the variations in ρ. Nimmer *et al.* [10] have shown this to hold true for the 5% and 15% density reduction materials, and also that E_{TR} and E_{BR} correlate extremely well with ρ.

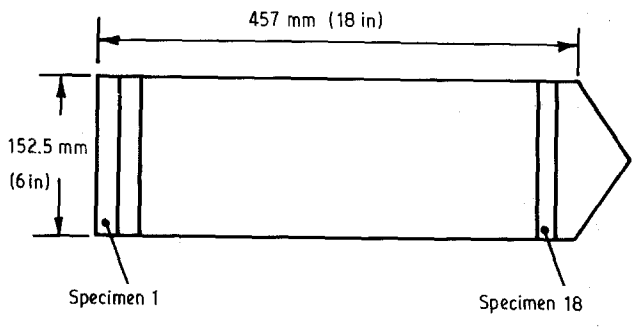

Figure 1 Numbering scheme for test specimens cut from edge-gated structural foam plaque.

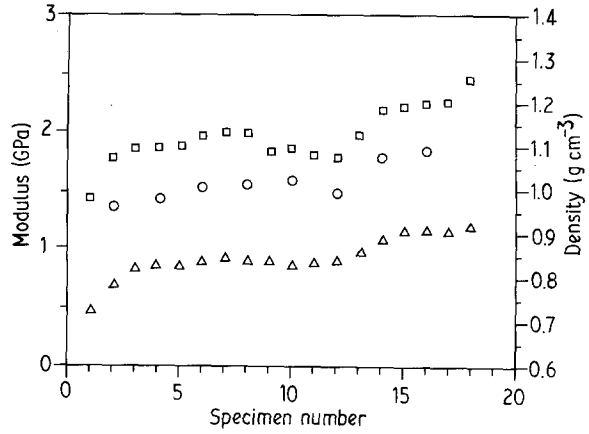

Figure 2 Variations of the (△) average local density, ρ, and the (□) bending, E_{BR}, and (○) tensile, E_{TR}, moduli of rectangular specimens cut from a 25% nominal density reduction, 6.35 mm thick edge-gated foam plaque.

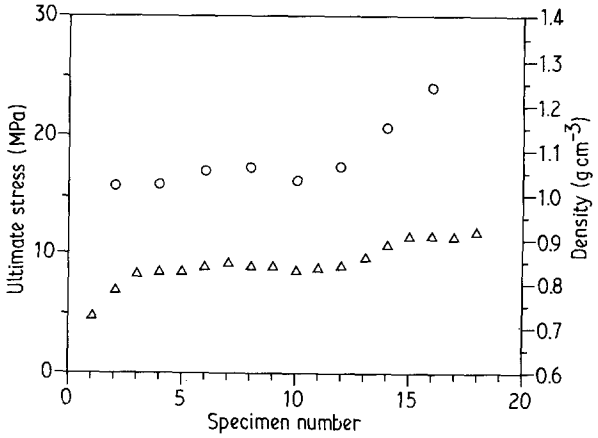

Figure 3 Variations of the (△) average local density, ρ, and (○) ultimate stress, σ_0, in rectangular specimens cut from a 25% nominal density reduction, 6.35 mm thick edge-gated foam plaque.

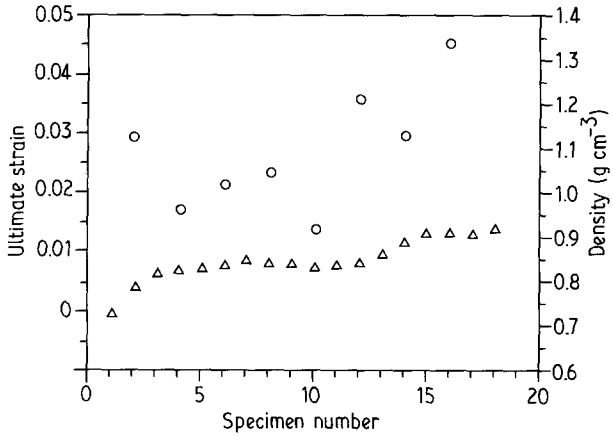

Figure 4 Variations of the (△) average local density, ρ, and (○) ultimate strain, ε_0, in rectangular specimens cut from a 25% nominal density reduction, 6.35 mm thick edge-gated foam plaque.

The variations of the ultimate stress, σ_0, and the ultimate strain, ε_0, along the plaque are shown, respectively, in Figs 3 and 4, in which the density variation is also shown for comparison. Clearly, σ_0 and ε_0

have very large variations across the plaque. Here again, the ultimate stress appears to track the specimen density, but there is more scatter in the ultimate strain.

Nimmer *et al.*'s data [10] show that ρ, E_{TR}, E_{BR}, and σ_0 have much smaller variations along a 5% density reduction plaque and, for all practical purposes, they can be assumed to be uniform. The variations in the properties of the 15% density reduction material [10] are smaller than those of the 25% density reduction material discussed above. Clearly, the ultimate strengths and strains of specimens cut from 25% density reduction parts should be expected to show larger variations, whereas the variations in specimens from 5% density reduction material should be quite small.

Because of the large density variations across plaques, regions in 15% and 25% density reduction materials can have the same density and therefore the same mechanical properties. The complexity of structural foams can be further gauged from the foam morphologies of the fracture surfaces of tensile bars for 5%, 15% and 25% density reduction materials shown in Fig. 5. The pictures for each density reduction are for different specimens from the same plaque; moulding occurred from the right to the left. Clearly, the foam morphology changes across the plaque. These changes are more significant for the higher density reduction materials. While there are some similarities between the morphologies of the 15% and 25% density reduction materials, the morphology of the 5% density reduction material is quite different.

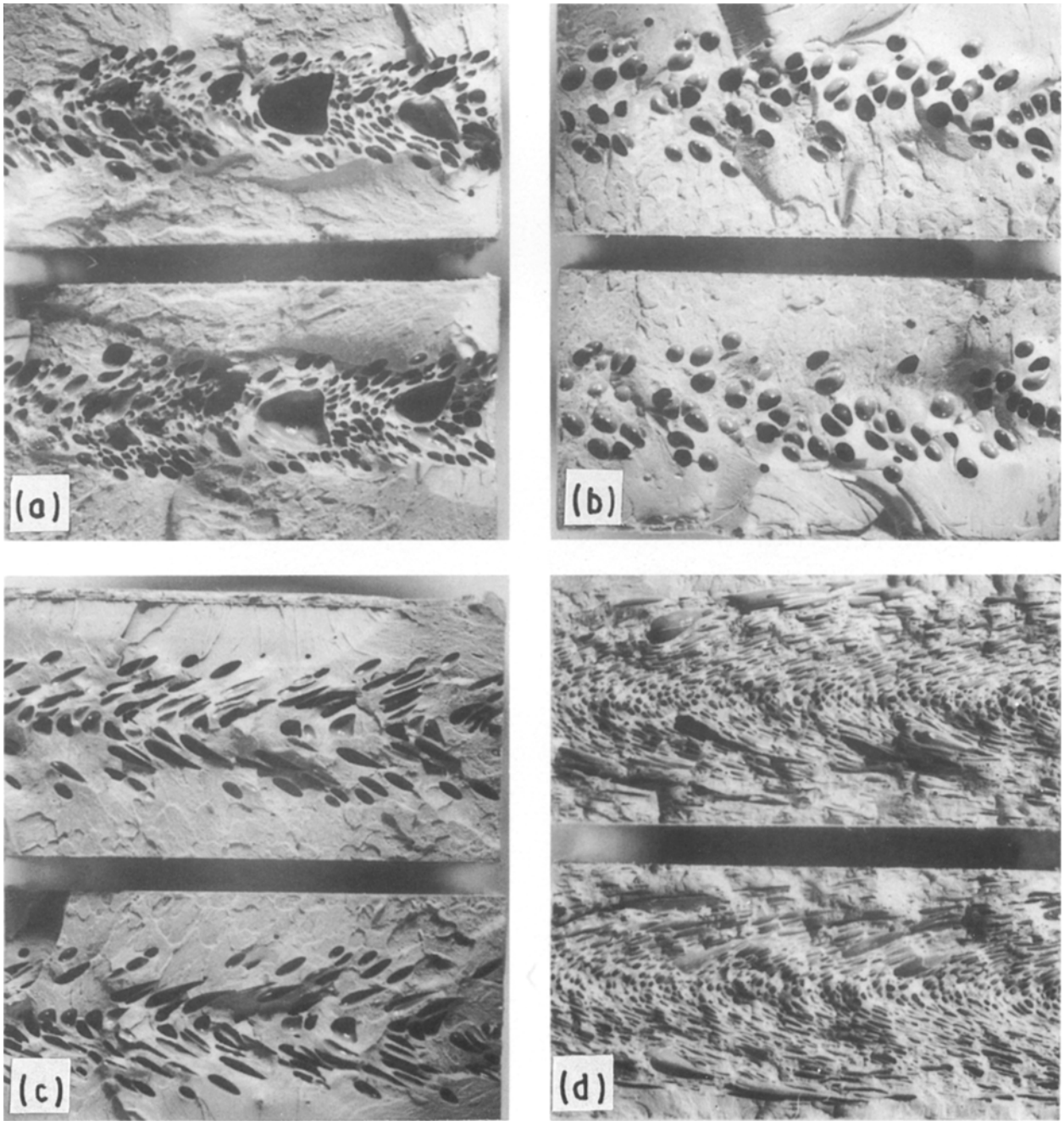

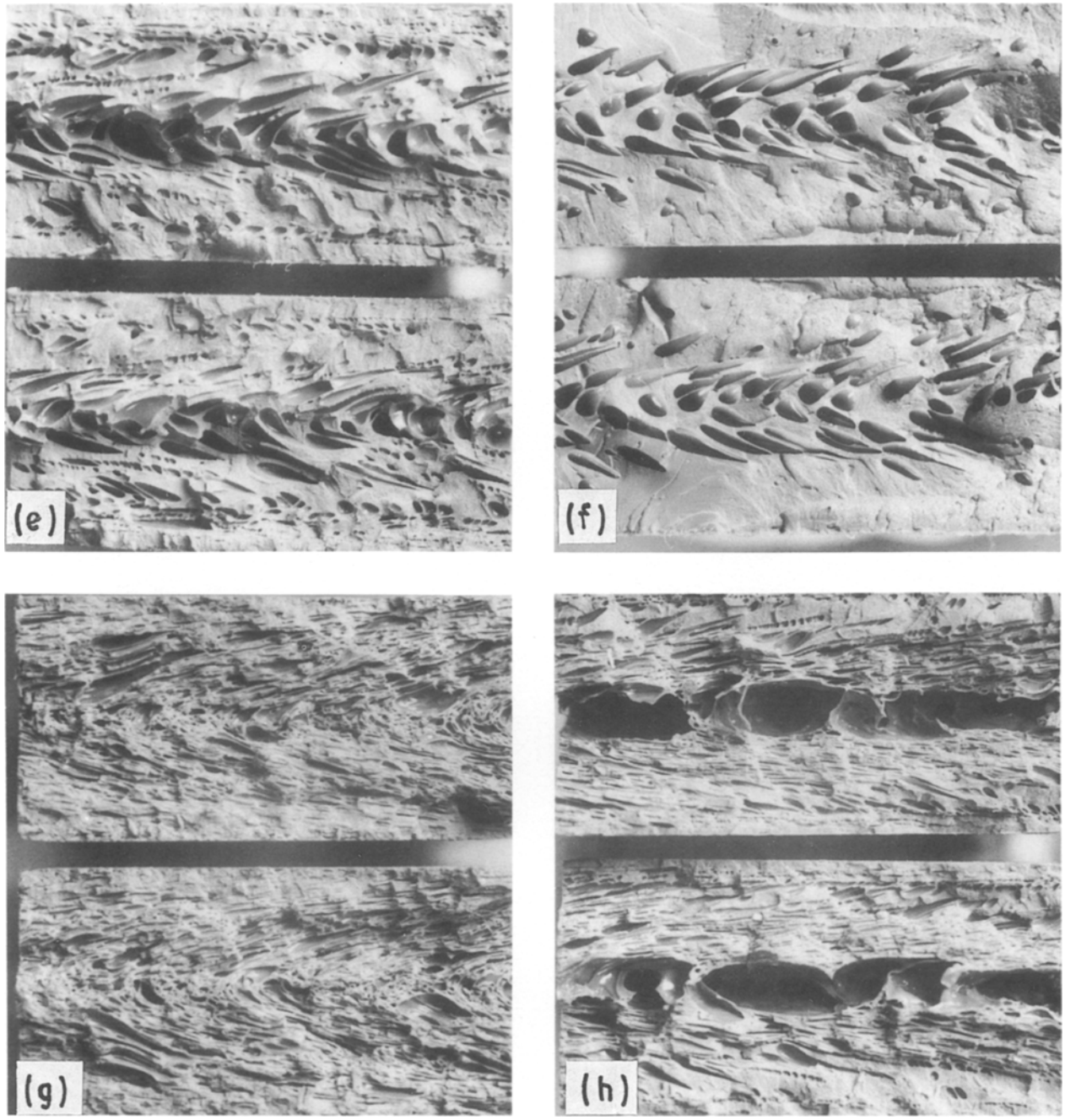

Figure 5 Morphologies of the fracture surfaces of tensile test bars for (a–c) 5%, (d–f) 15% and (g–i) 25% nominal density reduction materials. The pictures for each of the three density reductions are for different specimens from the same plaque. (a) Specimen 1, $\rho = 1.00$; (b) Specimen 12, $\rho = 1.02$; (c) Specimen 18, $\rho = 1.01$; (d) Specimen 3, $\rho = 0.88$; (e) Specimen 9, $\rho = 0.94$; (f) Specimen 12, $\rho = 0.98$; (g) Specimen 3, $\rho = 0.82$; (h) Specimen 13, $\rho = 0.86$; (i) Specimen 17, $\rho = 0.91$.

3. Vibration welding

For a neat thermoplastic resin, a typical vibration weld has the four phases [1, 2] schematically shown in Fig. 6. In the first phase, Coulomb friction generates heat at the interface, raising its temperature to the point at which the polymer can undergo viscous flow. In the second phase, the interface begins to melt and the mechanism of heat generation changes from solid Coulomb friction to dissipation in the molten polymer. The molten polymer begins to flow in a lateral

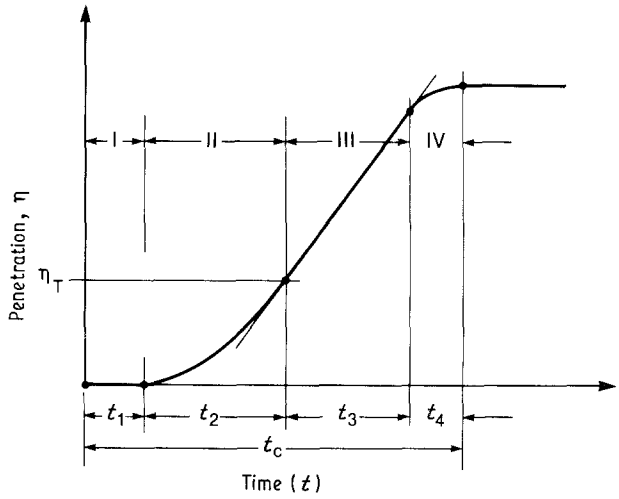

Figure 6 Schematic penetration–time curve showing four phases of the vibration welding process.

direction, resulting in an increase in the weld penetration – the distance by which the parts approach each other as a result of lateral flow. In the third phase, the melting and flow are at a steady state, and the weld penetration increases linearly with time. When the machine is shut off, the weld penetration continues to increase because the weld pressure causes the molten film to flow until it solidifies. This is phase four.

4. Test procedure

Twelve test specimens were cut from 152.5 mm × 457 mm (6 in × 18 in) edge-gated moulded plaques, with the flow direction along the length, as per the layout shown in Fig. 7. The edges of each specimen were machined to obtain rectangular blocks of size 76.2 mm × 25.4 mm × 6.35 mm (3 in × 1 in × 0.25 in) to ensure accurate alignment of the surfaces during butt welding. The specimens were numbered, with Specimen 1 being closest to the gated edge. At each location (specimen number), appropriate edges of specimens were marked A, B, C and D to identify interior and exterior edges. Welds of surfaces B to C would then correspond to welding of foamed material from the same region. Of course, edges A and D, whose surfaces are not machined, have thick skins. (Note that the 12 weld specimens shown in Fig. 7 were 25.4 mm wide, whereas the 18 tensile-test specimens marked in Fig. 1 were only 19.05 mm wide. Also note the different numbering schemes used: while in Fig. 7 Specimen 1 is closest to the gated edge, in Fig. 1 Specimen 1 is furthest from the gated edge.)

Details of the weld procedure have been described previously [3]. Two specimens with machined lateral edges were vibration welded along 25.4 mm × 6.35 mm edges resulting in a 152.4 mm × 25.4 mm × 6.35 mm (6 in × 1 in × 0.25 in) bar, which was then routed down to a standard ASTM D638 tensile test specimen with the vibration-welded butt joint in its centre, as shown in Fig. 8. These bars were then subjected to a constant displacement rate tensile test corresponding to a nominal strain rate of $10^{-2}\,s^{-1}$.

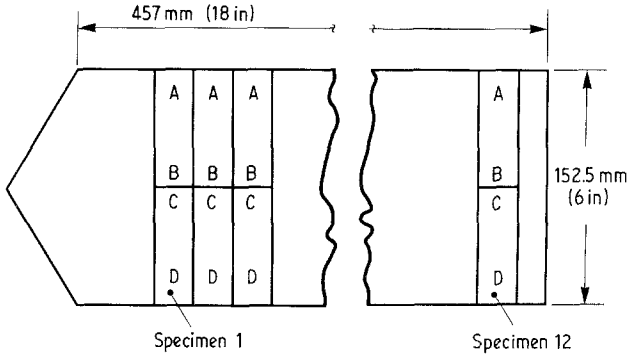

Figure 7 Layout showing where weld specimens were cut from 152.4 mm × 457.2 mm M-PPO-SF moulded plaques.

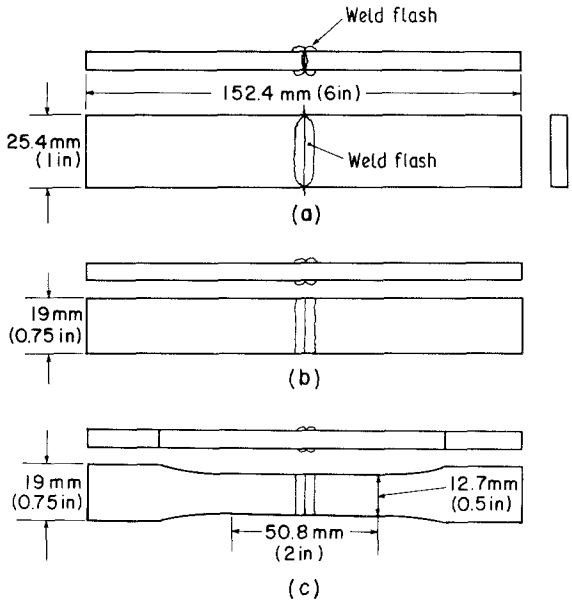

Figure 8 Geometry of specimens for determining the strength of butt welds.

During each strength test, the average strain across the weld interface was measured with a 25.4 mm (1 in) gauge length extensometer. Because of the local nature of failure, this extensometer only establishes the lower limit of the strain at failure; the actual strain can be much higher in many cases.

5. Process phenomenology

The penetration–time curves for the 5% and 25% density reduction foams, at weld pressures of 0.52 MPa (75 p.s.i.) and 0.9 MPa (130 p.s.i.) are shown in Fig. 9. They exhibit the four phases that are typical for neat resins. Clearly, for the same weld conditions, each of the four phases is shorter for the higher density reduction (25%), and the steady-state penetrations rates are higher. This is consistent with the higher levels of porosity at higher density reductions. Steady-state penetration data are listed in Table I, in which $\dot{\eta}$ is the steady-state penetration rate and η_c is the penetration that occurs during phase four. (With reference to Fig. 7, the last column in this table shows the location in the plaque from which a particular weld specimen was cut.)

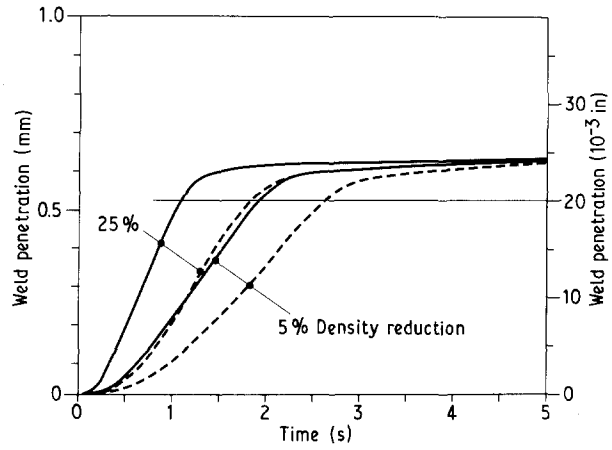

Figure 9 Penetration–time curves for 5% and 25% density reduction foams at weld pressures of (– – –) 0.52 and (———) 0.9 MPa. n = 120 Hz, a = 1.59 mm (0.0625 in).

6. Strength of structural foam welds

Table II gives strength data for 120 Hz welds of M-PPO-SF, at density reductions of 5% and 25%, for a weld amplitude of a = 1.59 mm at two different pressures. (The last column in this table shows the location in the plaque from which a particular weld specimen was obtained.) During welding, the vibratory motion was stopped at penetrations of 0.25 mm (0.01 in) and 0.51 mm (0.02 in). Because the molten film continues to flow outward during phase 4, the final penetration, η_F, is larger than these values. The excess corresponds to the penetration η_c, which is of the order of 0.1 mm (0.004 in), that is listed in Table I. t_0 is the time during which the specimens were subjected to vibratory motion. Note that these tests were done on eight sets of specimens, 1–4, from the gated-end region.

All the four 5% density reduction foam specimens failed at the weld. One out of the four 25% density reduction foam specimens did not fail at the weld. The weld strength, σ_w, is uniformly high, as are the corresponding strains to failure, ε_0. Apparently, full weld strength is attained even at penetrations as low as 0.25 mm (0.01 in). It would appear that lower weld pressures result in higher weld strengths, just as in solid M-PPO [4]. However, the effect is not as large as in solid M-PPO. The uniformity in the strengths is consistent with the uniformity in the strengths of tensile-test specimens cut from different parts of a plaque [10].

Strength data for structural foams are known to exhibit more scatter than those for neat resins (see Section 2 and [10]). In order to check for specimen-to-specimen consistency, and also to investigate the effects of larger penetrations, four tests were done at each of two penetrations of 0.64 mm (0.025 in) and 1.27 mm (0.050 in) on specimens 1–8. The results of these eight tests are listed in Table III. Only two specimens did not fail at the weld. Note that these specimens were cut by a saw and, as such, the weld surfaces may not initially have been as well aligned as the machined surfaces used in the tests listed in Table II. However, at the large penetrations (0.64 and 1.27 mm) used, any initial mismatch would be quickly evened out; this initial mismatch may explain some of the variability in the values of t_0 listed in Table III. Given the variability in the morphology of structural foams, the consistency in the strengths of these eight welds, all of which failed at the welds, is quite remark-

TABLE I Steady-state penetration rate and phase four penetration data for n = 120 Hz, a = 1.59 mm (0.0625 in) welds of 5% and 25% density reduction M-PPO-SF

Density reduction	p_0		$\dot{\eta}$		η_c		Specimen number
(%)	(MPa)	(10^3 p.s.i.)	(mm s^{-1})	(10^{-3} in s^{-1})	(mm)	(10^{-3} in)	
5	0.52	75	0.28	11	0.13	5	3
5	0.9	130	0.36	14	0.11	4.5	4
25	0.52	75	0.40	15.7	0.10	4	3
25	0.9	130	0.56	22	0.10	4	4

TABLE II Strength and ductility data for n = 120 Hz, a = 1.59 mm (0.0625 in) welds of 5% and 25% density reduction M-PPO-SF

Density reduction	p_0		η_F		t_0	η_c		σ_w		ε_0	Specimen number
(%)	(MPa)	(p.s.i.)	(mm)	(10^{-3} in)	s	(mm)	(10^{-3} in)	(MPa)	(10^3 p.s.i.)	(%)	
5	0.52	75	0.34	13.5	2.08	0.09	3.5	31.9	4.62	2.04	1
5	0.52	75	0.64	25	2.71	0.13	5	30.8	4.47	1.85	3
5	0.9	130	0.33	13	1.35	0.08	3	31.0	4.50	1.74	2
5	0.9	130	0.62	24.5	1.99	0.11	4.5	30.2	4.38	1.67	4
25	0.52	75	0.34	13.5	1.44	0.09	3.5	25.0	3.62	1.75	1
25	0.52	75	0.62	24.5	1.95	0.11	4.5	24.3	3.53	2.49[a]	3
25	0.9	130	0.33	13	0.83	0.08	3	22.3	3.24	1.36	2
25	0.9	130	0.62	24.5	1.18	0.11	4.5	20.3	2.94	2.30	4

[a] Specimen did not fail at the weld.

TABLE III Strength and ductility data for $n = 120$ Hz, $a = 1.59$ mm (0.0625 in), $p_0 = 0.9$ MPa (130 p.s.i.), welds of 5% density reduction M-PPO-SF

η_F		t_0	η_c		σ_w		ε_0	Specimen number
		s					%	
(mm)	(10^{-3} in)		(mm)	(10^{-3} in)	(MPa)	(10^3 p.s.i.)		
0.71	28.1	3.07	0.08	3.1	32.0	4.64	4.29[a]	5
0.75	29.4	2.26	0.11	4.4	32.1	4.65	2.08	6
0.71	27.8	2.88	0.07	2.8	31.0	4.50	4.34[a]	7
0.72	28.2	2.17	0.08	3.2	31.8	4.61	2.13	8
1.40	55	3.72	0.13	5	31.2	4.52	2.34	1
1.37	53.8	3.67	0.10	3.8	31.9	4.62	1.78	2
1.36	53.7	3.73	0.09	3.7	31.3	4.54	1.76	3
1.35	53.3	4.42	0.08	3.3	31.3	4.54	1.66	4

[a] Specimen did not fail at the weld.

TABLE IV Strength and ductility data for $n = 120$ Hz, $a = 1.59$ mm (0.0625 in) foam-surface to skin welds of 5% and 25% density reduction M-PPO-SF

Density reduction	p_0		η_F		t_0	η_c		σ_w		ε_0	Specimen number
					s					(%)	
(%)	(MPa)	(p.s.i.)	(mm)	(10^{-3} in)		(mm)	(10^{-3} in)	(MPa)	(10^3p.s.i.)		
5	0.52	75	0.36	14	2.13	0.10	4	31.6	4.58	1.60[a]	1
5	0.52	75	0.36	14	2.38	0.10	4	33.0	4.78	2.00	6
5	0.52	75	0.36	14	1.90	0.10	4	30.1	4.36	1.96[a]	12
25	0.52	75	0.37	14.5	1.45	0.11	4.5	21.9	3.18	1.84	1
25	0.52	75	0.38	15	1.47	0.13	5	18.4	2.67	1.92[a]	6
25	0.52	75	0.38	15	1.10	0.13	5	15.2	2.21	2.28[a]	12

[a] Specimen did not fail at the weld.

able, especially because the specimens were cut from very different regions of the plaque. Although the strains at failure appear to be somewhat larger for the lower (0.64 mm) welds, this could easily be ascribed to where in the moulded plaque these specimens were cut from. These strength values are also consistent with the 5% density reduction data in Table II. Stress–strain curves for 5% density reduction foam, as well as those for the welds, indicate a slight load drop off at strains above about 2%. As such, the weld strength of a 5% density reduction welded foam specimen that fails at a strain above 2% can be regarded to be equal to the strength of the structural foam. The data in Tables II and III then imply that welds on 5% density reduction foams have strengths that are comparable to those of the parent structural foam.

The strengths of the 25% density reduction foam welds exhibit greater variability, but this is consistent with the variability in the strength of the parent 25% density reduction material: weld specimens 1–4 in Fig. 6 correspond approximately to tensile-test specimens 18–14 in Fig. 1 in which the strength decreases away from the gated edge (see Fig. 3). Weld pressure appears to have a larger effect than in the 5% density reduction material. Here again, stress–strain curves indicate a load drop off at strains of the order of 2%. Because of this, although the weld strength in the four specimens appears to be the lowest (20.3 MPa) for $p_0 = 0.9$ MPa and $\eta_F = 0.62$ mm, the large strain at failure (2.3%) indicates that the weld strength is about as high as the strength of the local material.

In order to assess the weldability of the moulded foam skin to cut foam surfaces, strength tests were also done on specimens in which the skin surfaces A (see Fig. 7) were welded to foam surfaces C. The specimens (1, 6 and 12) were cut from the two ends and the middle of plaques. Strength data for A to C surface welds of 5% and 25% density reduction material, for $n = 120$ Hz, $a = 1.59$ mm and $p_0 = 0.52$ MPa, are listed in Table IV. A comparison with the data in Table II shows that the weld strength of A to C welds of the 5% density reduction material is comparable to B to C welds, if not higher. In comparison to the strengths of the B to C welds, the apparently lower strengths of the A to C welds of the 25% density reduction material can be ascribed to the inherent variability in the strength of this material shown in Fig. 3 (strains to failure are higher for the A to C welds) – weld specimens 6 and 12 (Fig. 7) correspond approximately to specimens 9 and 2 in Fig. 1 – and does not imply an actual reduction in weld strength.

7. Weld morphology

The morphologies of both faces of the 6.35 mm × 12.7 mm (0.25 in × 0.5 in) fracture surface of a 5% density reduction welded specimen ($p_0 = 0.52$ MPa, $\eta_F = 0.64$ mm; Specimen 3, second row in Table II) that failed at the weld are shown in Fig. 10. The bulk of the fracture surface has the texture of the fracture surface for a solid resin. There is little evidence of

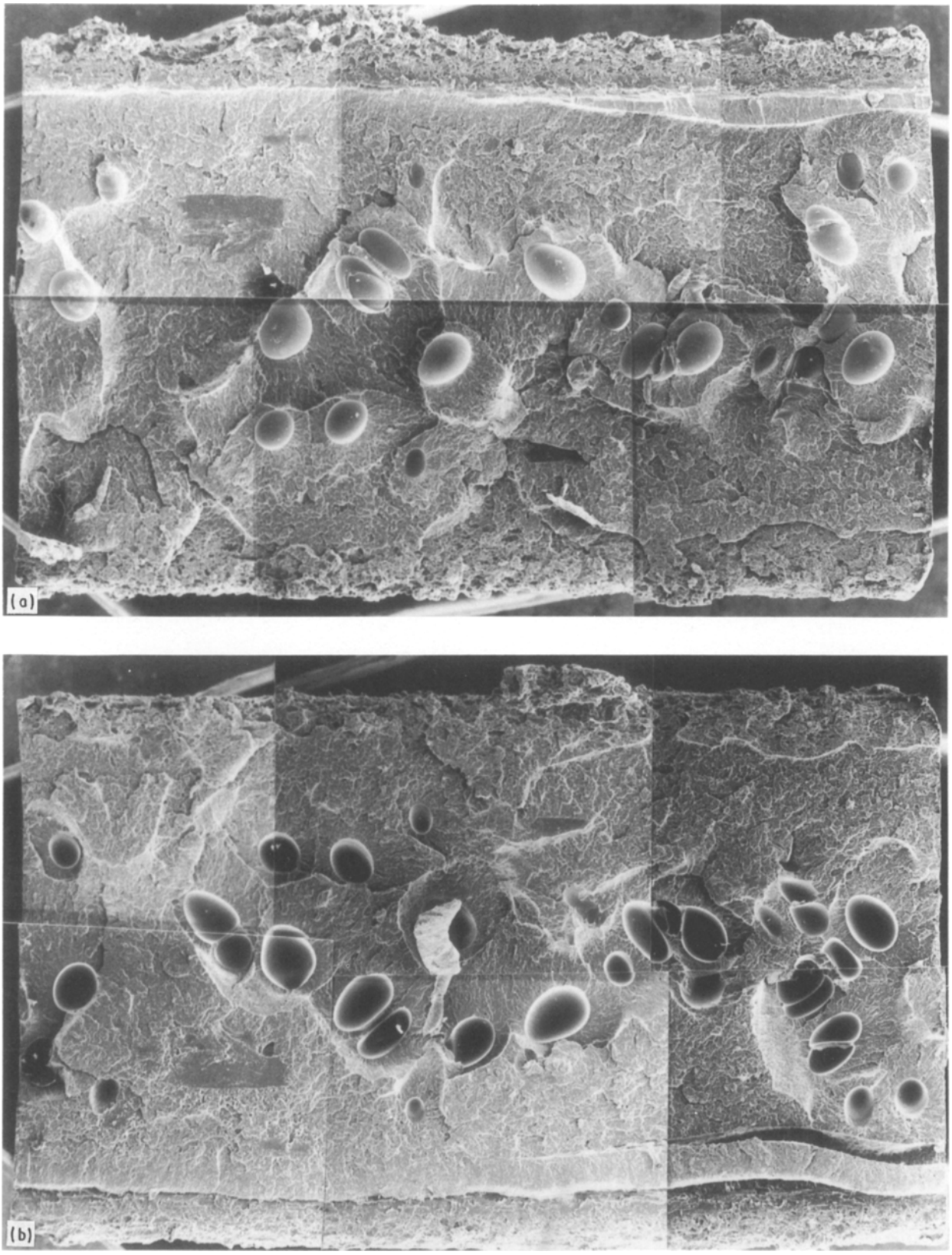

Figure 10 Fracture surfaces (6.35 mm × 12.7 mm) of a 5% density reduction M-PPO-SF welded specimen (Specimen 3: $p_0 = 0.52$ MPa, $\eta_F = 0.64$ mm).

macroscale porosity that 5% density reduction foam should have; the bulk of the pores fused during the welding process. The shiny globular protrusions (Fig. 10a) of the specimen represent molten material that flowed into corresponding cavities (Fig. 10b) in the second half of the specimen. The bulk of this flow probably occurred during phase 4. The shiny texture of the protrusions indicates that the molten material did not bond to the surface of the mating cavity. There could be two reasons for this. First, the amount of material forced into a cavity was not sufficient to fill it. Second, by the time the melt front advanced to the

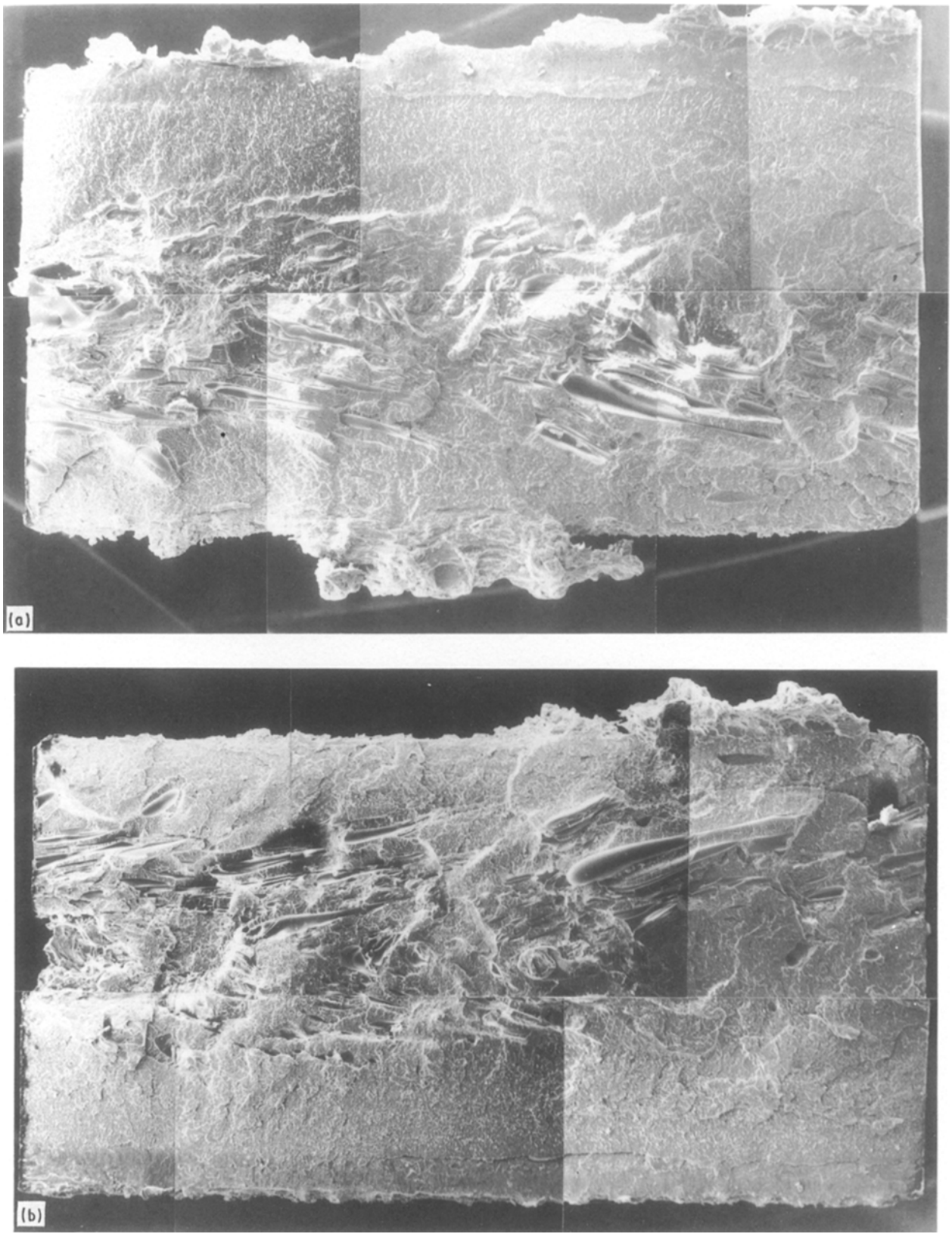

Figure 11 Fracture surfaces (6.35 mm × 12.7 mm) of a 25% density reduction M-PPO-SF welded specimen (Specimen 2: $p_0 = 0.9$ MPa, $\eta_F = 0.33$ mm).

cavity surface, the melt front had cooled off sufficiently to prevent bonding.

The morphology of the 6.35 mm × 12.7 mm fracture surface of 25% density reduction weld specimens is quite different. This can be seen from micrographs (Fig. 11) of both faces of the fracture surface of a welded specimen ($p_0 = 0.9$ MPa, $\eta_F = 0.33$ mm; Specimen 2, seventh row in Table II) that failed at the weld; the protrusions are elongated bubbles. The fracture surface has a surprisingly small number of bubbles for a 25% density reduction foam, which could reflect a higher local foam density. Fig. 12 shows

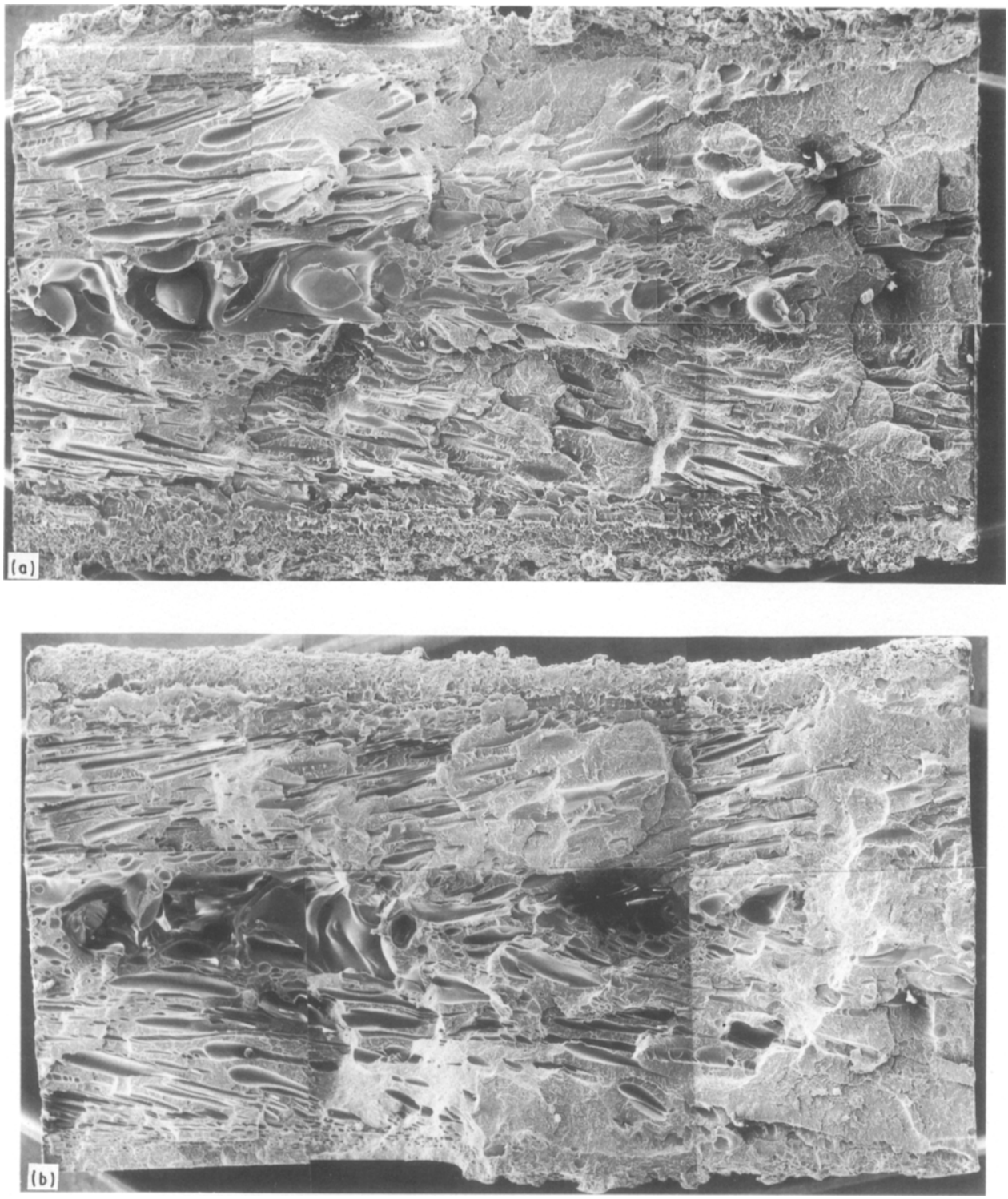

Figure 12 Fracture surfaces (6.35 mm × 12.7 mm) of a 25% density reduction M-PPO-SF welded specimen (Specimen 4: $p_0 = 0.9$ MPa, $\eta_F = 0.62$ mm).

the fracture surface of a higher penetration weld ($p_0 = 0.9$ MPa, $\eta_F = 0.62$ mm; Specimen 4, eighth row in Table II). Large numbers of elongated bubbles associated with high density reduction foams can be seen.

8. Conclusion

Clearly, M-PPO structural foam welds well. Although most of the test specimens failed at the welds, the weld strength was comparable to that of the foam, and the strains at failure were uniformly high. Under the right conditions, weld strengths equal to that of the foam should easily be attainable. This has also been shown to be true of foam-skin to foam welds.

The weld process phenomenology for foams is identical to that for all neat resins, including solid M-PPO: the penetration–time curves exhibit all the four phases of vibration welding. Although lower weld pressures appear to result in slightly higher weld strengths, the effect of pressure is not as significant as in the welding of solid M-PPO, for which increases in

weld pressure cause a significant decrease in weld strength.

On the basis of the data in this paper it would appear that when foams are welded along the moulded skin surface, as opposed to the cut specimens used in this study, the weld strength would be even higher.

Acknowledgements

Support provided by GE Plastics is gratefully acknowledged. The contributions of K. R. Conway, who carried out all the tests, are greatly appreciated. Special thanks are due to Julia A. Kinloch for her help and patience during the preparation of this paper.

References

1. V. K. STOKES, *Polym. Engng Sci.* **28** (1988) 718.
2. *Idem, ibid.* **28** (1988) 728.
3. *Idem, ibid.* **28** (1988) 989.
4. *Idem, ibid.* **28** (1988) 998.
5. *Idem, ibid.* **29** (1989) 1683.
6. V. K. STOKES and S. Y. HOBBS, *ibid.* **29** (1989) 1667.
7. S. Y. HOBBS and V. K. STOKES, *ibid.* **31** (1991) 502.
8. V. K. STOKES, *ibid.* **31** (1991) 511.
9. V. K. STOKES, R. P. NIMMER and D. A. YSSELDYKE, *ibid.* **28** (1988) 1491.
10. R. P. NIMMER, V. K. STOKES and D. A. YSSELDYKE, *ibid.* **28** (1988) 1501.
11. J. L. THRONE, *Plast. Des. Process.* **16**(9) (1976) 20.
12. R. C. PROGELHOF and K. EILERS, "Apparent Modulus of a Structural Foam Member", paper presented at SPE Engineering Properties and Structure DIVTEC III, "Processing for Properties", Woburn, MA (1977) Proceedings, Society of Plastics Engineers, Brookfield, CT.
13. J. L. THRONE, *J. Cell. Plast.* **14** (1978) 21.

Received 28 May
and accepted 2 October 1991